

THE ORIGIN OF THE NARROW LINE REGION OF MRK 3: AN OVERPRESSURED JET COCOON ¹

A. Capetti

*Osservatorio Astronomico di Torino
Strada Osservatorio 20, 10025 Torino, Italy*

D.J. Axon²

*Division of Physical Sciences, University of Hertfordshire
College Lane, Hatfield, Herts AL10 9AB, U. K.*

F.D. Macchetto²

*Space Telescope Science Institute
3700 San Martin Drive, Baltimore, MD 21218*

A. Marconi

*Osservatorio Astrofisico di Arcetri
Largo E. Fermi 5, 50125, Firenze, Italy*

C. Winge³

*Instituto de Física
Universidade Federal do Rio Grande do Sul, Av. Bento Gonçalves
9500, C.P. 15051, CEP 91501-950, Porto Alegre, RS, Brazil.*

ABSTRACT

We have obtained HST FOC f/48 long-slit optical spectroscopy of the inner 2'' of the Narrow Line Region of the Seyfert 2 galaxy Mrk 3 with a spatial resolution of 0''.06. Spectra were taken in six locations with the slit approximately perpendicular to the radio-axis.

In the region cospatial with the radio-jet, where the brightest emission line knots are located, the velocity field is highly perturbed and shows two velocity systems separated

¹Based on observations with the NASA/ESA Hubble Space Telescope, obtained at the Space Telescope Science Institute, which is operated by AURA, Inc., under NASA contract NAS 5-26555 and by STScI grant GO-3594.01-91A

²Affiliated to the Astrophysics Division, Space Science Department, ESA

³CNPq Fellowship, Brazil

by as much as 1700 km s^{-1} . In several locations the split lines form almost complete velocity ellipsoids implying that we are seeing an expanding shell of gas. The diameter of this shell ($\sim 200 \text{ pc}$) is much larger than the width of the radio-jet ($d < 15 \text{ pc}$). We interpret this to be the consequence of the rapid expansion of a cocoon of hot gas, shocked and heated by the radio-emitting outflow, which compresses and accelerates the ambient gas. The cocoon mediates the energy exchange between jets and line emitting gas. The gas motions within the NLR of Mrk 3 are therefore clearly dominated by the interaction between the jets and the interstellar medium and the NLR itself is essentially a cylindrical shell expanding supersonically.

With its current size of 200 pc the cocoon has expanded to several disk scale heights. Due to the external gas density stratification, the hot gas located above the plane of the disk blows out into the halo, puncturing the bubble and fracturing the velocity ellipsoids. The system is effectively momentum driven.

From the size and velocity of the expanding region, we derive an upper limit to the radio-source age, $\lesssim 1.5 \cdot 10^5$ years, and a lower limit for the jet power, $\gtrsim 2 \cdot 10^{42} \text{ erg s}^{-1}$, required to inflate the cocoon and estimate that the jet minimum advance speed is $3 \cdot 10^{-3} \text{ pc per year}$. The total kinetic energy of the high velocity gas associated with the radio-jet can be estimated as $\sim 6 \cdot 10^{54} \text{ erg}$, comparable to the total energy carried by the jet over its lifetime and this quantitatively supports the idea that the NLR gas is accelerated by the jet.

Radio-outflows are associated with at least 50 % of Seyferts galaxies with typical sizes smaller than a few kpc. If the advance speed of Mrk 3 is representative of the Seyfert population then these sources must also be short lived and probably recurrent. Evidence that this is indeed the case is provided by the fact that the expansion time-scale derived for NGC 1068 is comparable to that seen in Mrk 3.

The jet kinetic luminosity of Mrk 3 is between 2 and 3 orders of magnitude smaller than that derived for radio-loud AGNs with similar emission-line luminosity. On the other hand, the fraction of jet power dissipated in radio-emission is similar. We speculate that the main distinction between radio-quiet and radio-loud AGN is ascribed to a difference in jet power rather than to a different efficiency in synchrotron emission production.

Subject headings: Galaxies: individual (Mrk 3) — galaxies: Seyfert — galaxies: jets — galaxies: active

1. Introduction

During the last two decades ground based studies of Seyfert galaxies have firmly established that a close relationship exists between radio and line emission. In particular they showed that their Narrow Line Region (NLR) is inevitably cospatial with the radio-emission (e.g. Wilson & Ulvestad, 1983; Haniff, Wilson & Ward, 1988). Furthermore, galaxies harboring a linear radio source have unusually wide line profiles (Whittle 1985) and display a correspondence between the location of the high velocity NLR gas with that of the radio ejecta (e.g. Whittle et al. 1988; Baldwin, Wilson & Whittle 1987; Pedlar et al. 1989). This spatial and kinematical association has been interpreted as due to the compression and acceleration of the interstellar gas induced by the expansion of the radio-ejecta (Wilson & Willis 1980, Boller et al. 1982, Pedlar et al. 1989, Taylor et al. 1989, 1992).

Hubble Space Telescope (HST) allowed us for the first time to fully resolve the region from which the narrow emission lines originate. The results of extensive narrow-band imaging of Seyfert galaxies clearly showed that the NLR morphology is completely determined by the presence of radio outflows (e.g. Bower et al. 1994, 1995, Capetti et al. 1995a, 1995b, 1996, 1997a, 1997b, Falcke et al. 1996, 1998). In particular, Seyfert galaxies with a lobe-like radio morphology have bow shock shaped emission line regions while those with a jet-like radio structure have jet-like emission line structures. These observations provide further compelling evidence for strong dynamical interactions between the NLR gas and radio-emitting ejecta.

In this framework it is of great interest to study the effects of this interaction on the NLR dynamics at a high spatial resolution. This prompted a program of long-slit observations using the Faint Object Camera (FOC) in its spectrographic mode in order to study in detail the velocity field of the NLR of Seyfert galaxies.

The first results from observations of NGC 4151 (Winge et al. 1997, 1998) and NGC 1068 (Axon et al. 1998) show clear evidence that the highly perturbed and complex velocity field of the NLR of these objects is strongly influenced by the jets propagation. In particular, high velocity gas components are associated univocally with the jet region.

We now present the results of long-slit HST/FOC spectroscopy of Mrk 3, a Seyfert 2 galaxy which represents one of the clearest examples of close association between radio and line-emission. Radio-images show a linear structure extending over $\sim 2''$, dominated by two symmetric and highly collimated jets (Kukula et al. 1993). HST emission-line images of Mrk 3 revealed that its NLR has a striking “S” shaped morphology composed of a series of knots, sheets or filaments and is basically cospatial with the radio-jets (Capetti et al. 1995a, 1996).

In this paper we show that the NLR of Mrk 3 is essentially an expanding shell surrounding the radio-jet whose velocity field is determined by the energy input of the outflowing jets. The detailed spatial and velocity information derived allow us to investigate the energetics of the jet/NLR interaction and to set constraints on the properties and on the evolution of the radio-source associated to Mrk 3. We defer the discussion on line ratios and the ionization properties of the emitting gas to a forthcoming paper.

Throughout this paper we will adopt a recession velocity for Mrk3 of 4000 km s^{-1} ($z = 0.0133$) which, for $H_0 = 50 \text{ Km s}^{-1} \text{ Mpc}^{-1}$, yields a distance of 80 Mpc where $1''$ corresponds to 390 pc.

2. Observations and Data Reduction

Mrk 3 was observed using the FOC f/48 long-slit spectrograph on December 9th, 1996. One pixel corresponds to 1.78\AA and $0''.0287$ along the dispersion and slit directions, respectively. The F305LP filter was used to isolate the first order

spectrum which covers the 3650–5470 Å region and therefore includes the [O II]λ3727, Hβλ4861 and [O III]λλ4959, 5007 Å emission lines. An interactive acquisition 1024x512 zoomed image was obtained with the f/48 camera through the F342W filter to accurately locate the brightest line-emission regions. The slit, 0′′063x13′′5 in size, was placed at a position angle of -25°. Spectra with exposure times of 1000 seconds were taken in the 1024x512 non-zoomed mode at 7 locations separated by 0′′4. An additional spectrum of 780 s was taken immediately following the interactive acquisition image, before the telescope small angle maneuver (position 2 in Fig. 1).

The data reduction follows the procedure described in detail by Macchetto et al. 1997. In summary, all frames, including those used for subsequent calibrations, were geometrically corrected by using the equally spaced grid of reseau marks etched onto the first photocathode in the intensifier tube. Any remaining internal distortion was corrected tracing the spectra of two stars in the core of the globular cluster 47 Tuc. The distortion along the spatial direction was obtained in a similar way, tracing the brightness distribution of the emission lines of the planetary nebula NGC 6543. Observations of NGC 6543 were also used to obtain the wavelength calibration. The instrumental broadening is estimated to be $\sim 320 \pm 20$ km s⁻¹. Flux calibration was performed using the observations of the spectrophotometric standard star LDS749b.

To accurately determine the location of the slits we compared the surface brightness profile derived from the HST FOC, f/96, [O III] image of Capetti et al. (1996) with that measured from the spectra at the six slit positions which yielded useful data. The best match is displayed in Fig. 1 and is accurate to within half a slit width ($\simeq 0′′03$). The slit locations, identified as POS1 through POS6, cut across the emission-line region of MRK 3 in a direction almost perpendicular to that of the radio-axis, P.A. +84° (Kukula

et al. 1993).

3. Results

Velocities were derived by fitting gaussians profiles to the [O III] 5007λ line at each individual pixel using the task LONGSLIT in the TWODSPEC FIGARO package (Wilkins & Axon 1992). In several locations the line is composed of more than one component and in these cases multiple gaussian fitting was performed. In regions of low signal-to-noise, up to three pixels along the spatial direction were coadded. The resulting velocity profiles across the slit at each location are shown in Figs. 2 through 8, where we also plot line widths and intensities. The origin of the X-axis for each slit location is set at the intersection with the radio-axis.

3.1. Description of the individual spectra

- POS1: the line profiles are split into two distinct velocity systems in the region of the radio-jet, with a separation of ~ 1000 km s⁻¹. Toward the South, only the redshifted component is visible. The region of high velocity is extended over $\sim 0′′5$. The slit also crosses the bright Southeastern blob. This blob is detached from the main NLR structure and not directly associated with the radio-jet. The gas in this region has a velocity of ~ 3600 km s⁻¹ and is significantly blueshifted from the velocity on the East side of the NLR which is ~ 4300 km s⁻¹ (Wagner 1987, Metz 1998). Furthermore the lines are quite broad, ~ 700 km s⁻¹.
- POS2: this slit position was obtained during the interactive acquisition and was located close to POS1. On the North side of the NLR the velocity is approximately constant around 3900 km s⁻¹. Along the radio-axis there is a dramatic split of the lines with a separation which increases very rapidly and reaches a maximum of 1700 km s⁻¹. Unlike in POS1, the velocity field forms nearly a complete velocity ellipsoid. We

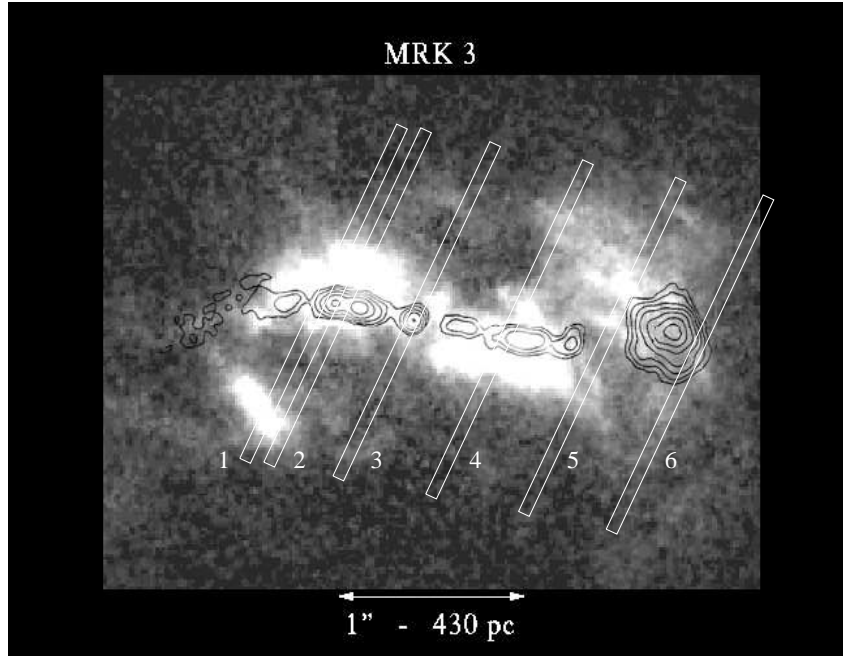


Fig. 1.— HST/FOC image of Mrk 3 in the [O III] emission line from Capetti et al. (1996) with superposed the contour radio image from Kukula et al. (1993) and the 6 slit positions where the FOC f/48 spectra were taken. North is up and East is to the left.

are seeing an expanding shell of size $\sim 0''.3$ around the radio-jet. The line widths of the individual components are always large, 500 km s^{-1} , and significantly wider than the instrumental broadening of 320 km s^{-1} . The large increase in line width just North of the split-line region is probably due to spatial confusion of the two velocity systems at the periphery of the shell. On the opposite side of the jet the slit grazes the bright SE blob. A smooth gradient of 200 km s^{-1} can be seen over a distance of $0''.4$ and, again, line widths are large $\sim 700 \text{ km s}^{-1}$.

- POS3: the slit is located on the brightest blob of the NLR of Mrk 3, close to its center of symmetry and, likely, to its hidden nucleus. The velocity field is remarkably flat on the blob but the lines are characteristically broad (500 km s^{-1}). The emission from this blob is redshifted by about $\sim 200 \text{ km s}^{-1}$ with respect to the galaxy systemic velocity. Immediately North of this blob, corresponding to where the radio-

jet intersects the slit, lines are again split in two components with a velocity separation of $\sim 1000 \text{ km s}^{-1}$.

- POS4: this location is symmetric to POS1 with respect to the nucleus and the velocity field is very similar but with a reversed symmetry. Again it shows a very large line splitting (1200 km s^{-1}) along the radio-jet over $\sim 0''.4$ in the form of a broken velocity ellipsoid.

- POS5: the gas kinematics are complex. Three highly perturbed regions correspond to three bright filaments crossed by the slit. The first, toward the South, is part of the main NLR structure. The remaining two, which are blueshifted by $\sim 600 \text{ km s}^{-1}$ and have large line widths, are associated with the radio-lobe. These structures are superposed onto a more regular pattern determined by the diffuse emission. Such complex line profiles has been seen previously on the lobe of the powerful radio-Seyfert IRAS 04210+0400

(Holloway et al. 1996).

- POS6: slit location 6 grazes the edges of the NLR and of the Western radio-lobe in a region of diffuse line emission. While the velocity field is essentially quiescent, with a dispersion of less than 250 km s^{-1} , the line profiles are significantly broad only in the region along the radio-axis, with a FWHM as high as 1000 km s^{-1} .

4. Kinematics of the NLR gas

The most dramatic result is that, kinematically, the NLR of Mrk 3 takes the form of a broken velocity ellipsoid centered on the radio-jet. This is the expected behaviour of an expanding cocoon of gas circumscribing the radio-jet and is unambiguous evidence that the NLR is created by the interaction of the radio-jet through the interstellar medium. Note that while there is a misalignment between the NLR and radio axis (Capetti et al. 1995a) the velocity ellipsoid is centered firmly on the jet. Line widths in the expanding regions are always broad, 500 km s^{-1} , suggesting significant turbulence within the cocoon.

The diameter of the emission line shell ($\sim 200 \text{ pc}$) is much larger than the radio-jet which is unresolved in the MERLIN images ($d < 15 \text{ pc}$). This is an indication that the radio-plasma does not interact *directly* with the line emitting gas. This is physically expected since for a shock velocity of $\gtrsim 1000 \text{ km s}^{-1}$ the post shock temperature will be of $\gtrsim 10^7 \text{ K}$ (Taylor et al. 1992). A hot high-pressure cocoon then develops around the advancing radio-jet and mediates the energy exchange between jets and line emitting gas. At these temperatures the main cooling mechanism is free-free radiation rather than line emission. Strong support for this interpretation is the direct detection of the ultraviolet counterpart to the Mrk 3 jet (Axon, Capetti & Macchetto 1998).

The excess pressure of the hot gas initially drives the supersonic NLR expansion. But, as we shall now explain, we believe that the NLR

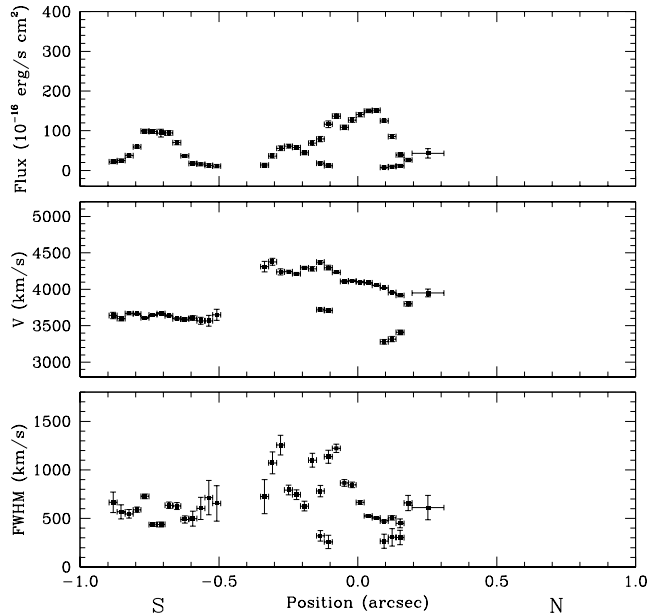


Fig. 2.— Intensity (upper panel), velocity (middle panel) and line widths (lower panel) measured at the slit position POS1.

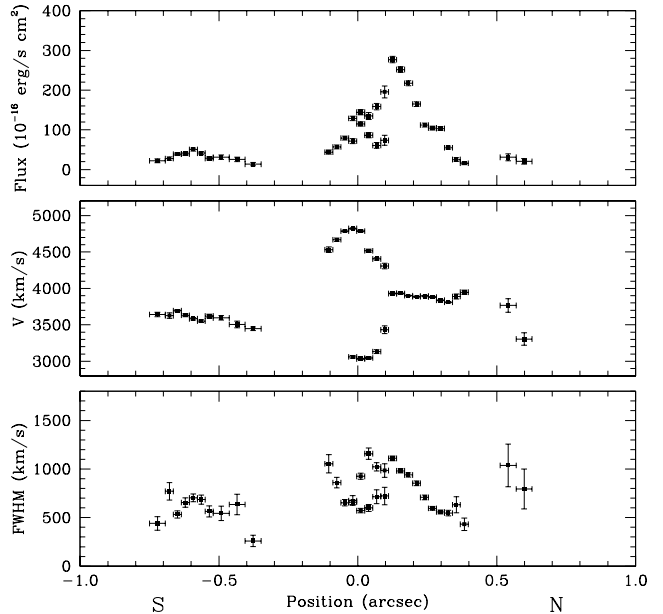


Fig. 3.— Same as Fig. 2 for slit position POS2.

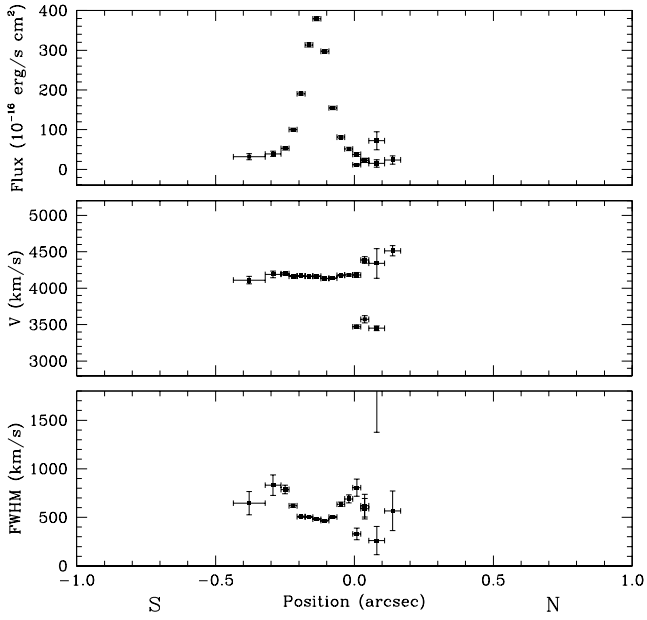


Fig. 4.— Same as Fig. 2 for slit position POS3.

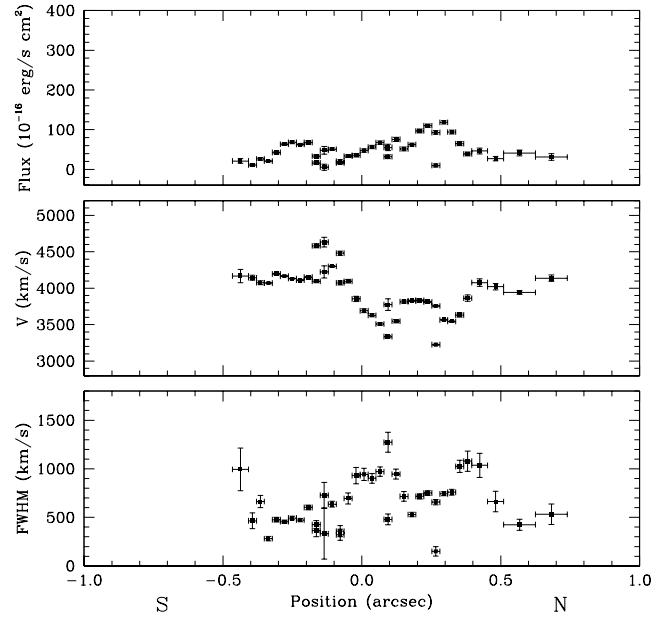


Fig. 6.— Same as Fig. 1 for slit position POS5.

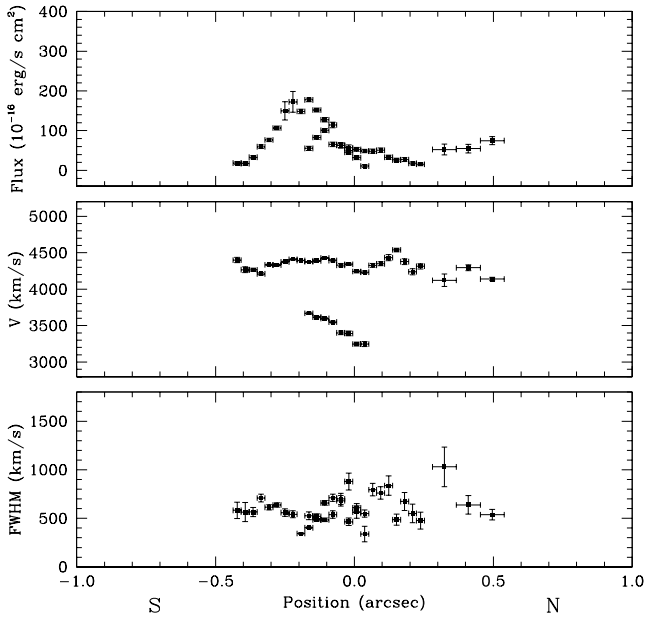


Fig. 5.— Same as Fig. 2 for slit position POS4.

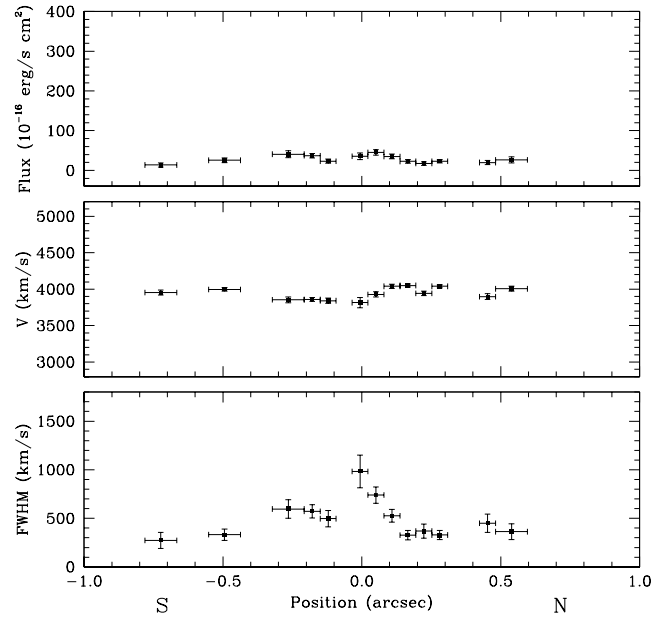


Fig. 7.— Same as Fig. 2 for slit position POS2.

is currently in a momentum driven phase as the bubble has been punctured. The two key facts leading to this conclusion are the mirror symmetry about the nucleus of the NLR emissivity and fractures in the velocity ellipsoids. As described above, on the Western jet the bubble is open towards the South and the peak of emission is to the North (POS1 and POS2) while the reverse is seen along the East jet (POS3 through POS5). This behaviour can be explained if the jets are propagating in the stratified gas of a disk galaxy and the jets are inclined with respect to the gas disk (see Fig. 8). The dynamical evolution is very similar to that of the wind driven superbubbles associated to OB associations or supernovae in the ISM (Tomisaka & Ikeuchi 1986, Mac Low & McCray 1988). Initially the bubble will expand asymmetrically with respect to the jet axis with the side away from the disk expanding more rapidly. It will still appear as a closed, although asymmetric, velocity ellipsoid. The bright emission line region corresponds to the side of the bubble which is snow-plowing into the disk. At this stage the NLR motions are pressure driven. When the bubble grows to be large enough it is more profoundly influenced by the stratification of the galactic disk. With the current size of 200 pc the cocoon has probably expanded to several disk scale heights and the hot gas located above the plane of the disk is blowing out into the halo, puncturing the bubble. At this time the system is effectively momentum driven.

Aside from the highly perturbed gas on which we have concentrated so far, at all slit locations there are extended regions in which the gas is relatively quiescent, i.e. with a velocity field characterized by small velocity gradients, small offset from the galaxy systemic velocity and relatively narrow line profiles. This gas is probably associated with the galaxy disk. The presence of an extended rotating gas disk in Mrk 3 is clearly seen in ground based data (Metz 1998) and it is normally observed in Seyfert galaxies. A similar two-components gas structure in the NLR has

been recently seen also in NGC 4151 (Winge et al. 1998). Radio outflows disrupt only locally the ordered rotation pattern.

5. Evolution of the cocoon

The evolution of an overpressured cocoon driven by a supersonic jet has been studied by several authors in the framework of powerful radio-galaxies. The same approach can be applied to the expanding cocoon in Mrk 3 but, in this case, we can directly measure its volume and expansion velocity which turn out to be crucial parameters to constrain the model.

Begelman & Cioffi (1989) showed that the evolution of a radio-source is determined by the balance between the ram pressure of the external medium with the thrust of the jet and, where the lateral expansion is concerned, with the cocoon internal pressure, i.e. $p_c \sim \rho_a v_{co}^2$, where p_c and v_{co} are the cocoon pressure and the present expansion velocity respectively and ρ_a is the external density. The medium in which the jet propagates is likely to be clumpy; a radio-source evolves within a non-uniform medium in a way similar to that with which it would interact with a smooth medium with the same average density (De Young 1993). In this situation the relevant value for ρ_a is the density averaged over the volume of the radio source.

The cocoon internal pressure is maintained by the energy carried by the jet. For a jet power L_j , averaged over the radio-source lifetime t_{rs} , we have $p_c \sim 2 t_{rs} L_j / V_c$. The cocoon volume, V_c , is given by $V_c \sim 2 d_c^2 l_c$ where d_c and l_c are its diameter and length.

The source age can be estimated noting that in such a cylindrical symmetry the expansion speed decreases as $t^{-1/2}$, i.e. $v_c = v_{co} (t/t_{rs})^{-1/2}$. Integrating the cocoon expansion from $t = 0$ to $t = t_{rs}$, i.e.

$$d_c \sim 2 \int_0^{t_{rs}} (t/t_{rs})^{-1/2} v_{co} dt \sim 4 v_{co} t_{rs} , t_{rs} \sim \frac{d_c}{4 v_{co}}$$

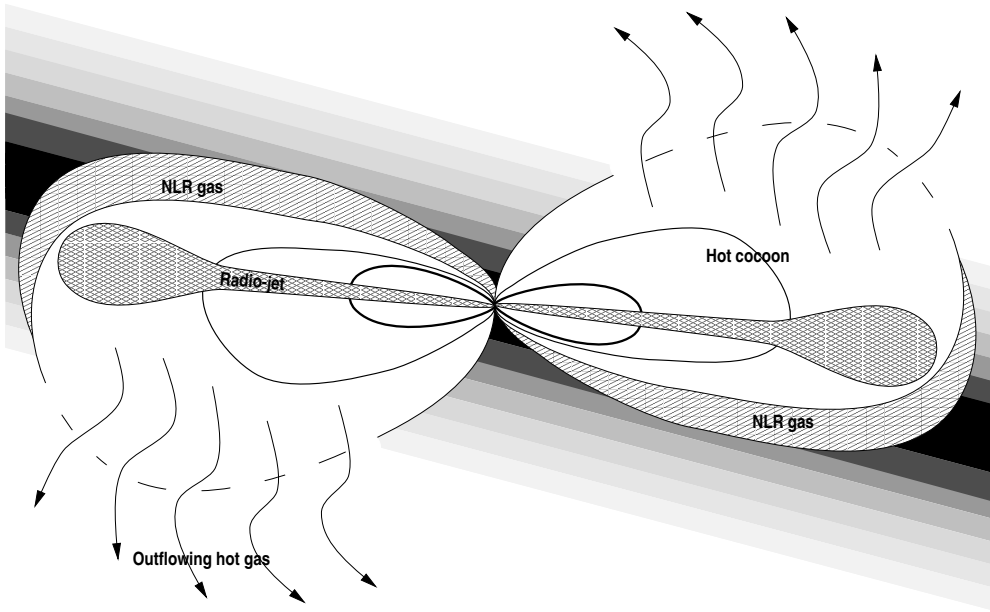


Fig. 8.— Cartoon illustrating the effects of the relative jet/disk orientation on the cocoon expansion and on the NLR morphology.

We can now express the jet power as

$$L_j \sim \rho_a v_{co}^2 d_c^2 l_c t_{rs}^{-1} \sim 4 \rho_a v_{co}^3 d_c l_c$$

Except for the external density ρ_a , the above parameters can be directly measured from our imaging and spectroscopy data of Mrk 3. We have $d_c \sim 200$ pc, $l_c \sim 500$ pc and $v_{co} \sim 700$ km s $^{-1}$ from which we get a jet power

$$L_j \sim 2 \cdot 10^{42} \rho_1 \text{ erg s}^{-1}$$

where ρ_1 is the average density of the unperturbed gas in units of one particle per cubic centimeter, a value which is appropriate to the interstellar medium of our galaxy (Cox & Reynolds 1987).

As for the radio-source age, the value which corresponds to the expansion law we adopted is $t_{rs} \sim 7 \cdot 10^4$ years. In reality the cocoon lateral evolution is very complex and depends on the precise distribution of the external medium and mass loading in the shell. The issue of mass load-

ing of astronomical flows has been discussed extensively in the literature (e.g. Hartquist et al. 1986) and it will be important in the evolution of the cocoon around the jet of Mrk 3. In addition the bubble has now been punctured and it is in a momentum driven phase. A firm upper limit of $1.5 \cdot 10^5$ years on the radio source dynamical time scale can be set by assuming a constant expansion at the present speed. On the other hand, a lower bound to the age of the outflow can be set if one assumes that the ionizing photons switch on at the same time as the radio-ejecta. The size of the Extended Narrow Line Region of Mrk 3 (~ 4 kpc, Pogge & De Robertis 1993) sets it to $\sim 10^4$ years. This would correspond to an expansion speed of less than $0.1 c$, similar to what is derived for powerful radio galaxies.

If the NLR dynamics are indeed dominated by the cocoon expansion the jet must have carried enough energy to accelerated the emitting gas. We can estimate the total kinetic energy of the high velocity gas, operatively defined as the

gas within $0''.2$ from the radio-jet with a velocity which differ by more than 300 km s^{-1} from the systemic velocity. A given $\text{H}\beta$ luminosity $L_{\text{H}\beta}$ corresponds to a mass of ionized gas (Osterbrock 1989)

$$M_{gas} \sim 7.5 \cdot 10^{-3} \frac{10^4}{n_e} \frac{L_{\text{H}\beta}}{L_{\odot}} M_{\odot}$$

Adopting an average $[\text{O III}]/\text{H}\beta$ ratio of 12.6 and an average density of 700 cm^{-3} (Metz 1998), an observed flux in the $[\text{O III}]$ line of $10^{-16} \text{ erg s}^{-1} \text{ cm}^{-2}$ corresponds to a mass of $\sim 130 M_{\odot}$. Integrating over the region of interest we find a total $[\text{O III}]$ flux of $4.3 \cdot 10^{-13} \text{ erg s}^{-1} \text{ cm}^{-2}$ (about 20 % of the total NLR emission) and a kinetic energy of $1.2 \cdot 10^{54} \text{ erg}$. Since only about 1/5 of the jet length is covered by our slits, the total kinetic energy of the gas associated with the radio-jet is $\sim 6 \cdot 10^{54} \text{ erg}$. On the other hand, during the radio-source expansion, half of the energy pumped by the jet goes into the cocoon's internal energy, while the other half goes into accelerating the external medium. This strictly applies only if the radiative losses of the cocoon are negligible. This is indeed the case since the cooling time for a temperature of 10^7 K is $\sim 1.5 \cdot 10^6 \rho^{-1}$ years, where ρ is the gas density, much longer than the radio-source dynamical time. The total energy deposited by the jet over the radio-source lifetime is $\sim 5 \cdot 10^{54} \text{ erg}$, remarkably similar to the kinetic energy of the line emitting gas. This provides *quantitative* support to the idea that the gas is accelerated (indirectly) by the jet.

6. Discussion

Radio outflows are known to be commonly associated with Seyferts galaxies: in at least 50 % of the cases the radio-emission is extended and often shows a linear structure (Ulvestad & Wilson 1989, Kukula et al. 1995) with typical sizes of less than $\sim 1 \text{ kpc}$ and they rarely extend beyond 3 kpc . For Mrk 3, we estimated that the radio source size has increased at a minimum speed of $\sim 3500 \text{ km s}^{-1}$ ($3 \cdot 10^{-3} \text{ pc}$ or $8 \mu\text{as}$ per year).

Recently, HST/FOC spectroscopy has been obtained also for NGC 1068 and NGC 4151 (Axon et al. 1998, Winge et al. 1997). The lateral expansion of the NLR gas in these two objects occurs at a similar speed to that in Mrk 3. In particular NGC 1068 shows a well developed jet-cocoon structure whose transverse size is $\sim 100 \text{ pc}$. The radio-source sizes of NGC 1068 and NGC 4151 are also comparable to that of Mrk 3 (900 and 600 pc respectively, Wilson & Ulvestad 1987, Pedlar et al. 1993) and we therefore naturally get similar dynamical timescales to that of Mrk 3. This suggests that the rate of linear size expansion of the radio-source of Mrk 3 is not unusually high, but is representative of Seyferts with linear radio-structures. If this is the case, the lifetime of radio outflows in Seyfert galaxies must be typically $\lesssim 10^5$ years, otherwise we should observe Seyfert radio sources extending well beyond 1 kpc . As a comparison, the source age for radio-galaxies ranges from 10^6 and 10^8 years (Alexander and Leahy 1987, Liu et al 1992, Parma et al. 1998). The longer timescales associated with radio-galaxies are also confirmed by the discovery of a line emitting expanding shell surrounding the jet of the 3C 120 which points an age for this source of $6 \cdot 10^6$ years (Axon et al. 1989). It appears that the phase of radio-activity in Seyferts is relatively short-lived.

Two alternative scenarios are viable at this stage. The high nuclear luminosity and the radio-activity are causally related and thus last for a similar time-scale in which case the whole Seyfert phenomenon is short-lived. The other possibility is that the radio activity in Seyferts is recurrent.

We can compare the radio, optical and jet luminosities of Mrk3 with those of other classes of active galactic nuclei. Its $[\text{O III}]$ luminosity is $L_{[\text{O III}]} = 2.1 \cdot 10^{42} \text{ erg s}^{-1}$ (Koski 1978) while the radio-luminosity at 4.8 GHz is $L_r = 2.7 \cdot 10^{30} \text{ erg s}^{-1} \text{ Hz}^{-1}$ (Ulvestad & Wilson 1984; Becker, White & Edwards, 1991) and $L_r = 2.4 \cdot 10^{31} \text{ erg s}^{-1} \text{ Hz}^{-1}$ at 178 MHz (Gower, Scott & Wills 1967). The integrated radio spectral in-

dex is then 0.66 and from which we derive a radio luminosity for Mrk 3 between 10 MHz and 100 GHz of $\sim 10^{41}$ erg s $^{-1}$.

The point representing Mrk 3 in the radio/optical luminosities plane falls within the region defined by the *radio-quiet* (RQ) quasars sample with $z < 0.5$ studied by Miller, Rawlings & Saunders (1991) which covers the range $10^{41} - 10^{44}$ erg s $^{-1}$ in line luminosity. Conversely, the radio luminosity, L_r of Mrk 3 is between 2 and 3 orders of magnitude below the average of the *radio-loud* (RL) AGN with similar line luminosities, L_{NLR} (Rawlings et al. 1989). The Mrk 3 jet power, L_j , (estimated from the expansion velocity of the emission line region associated with the radio-jet) can be compared with estimates based on the equipartition parameters (Rawlings & Saunders 1991) for RL AGNs. Mrk 3 lies again between 2 and 3 orders of magnitude below the region defined by the objects having similar values of L_{NLR} . On the other hand the ratio between L_j and L_r is similar for Mrk 3 and RL AGN, indicating that there is a similar fraction of jet power which is dissipated in radio-emission. More quantitatively, the efficiency at which the jet power is converted in radio emission in Mrk 3 is $0.05 \rho_1$. We speculate that the low radio-luminosity of radio-quiet objects is due to the presence of intrinsically less energetic outflows than in radio-loud objects, rather than to a lower efficiency in producing synchrotron emission. Clearly, observations of a sample of radio-quiet active nuclei with nuclear outflows are required before firm conclusions can be drawn.

7. Summary and conclusions

Our HST/FOC long-slit spectroscopic observations clearly show that the kinematics of the gas in the NLR of Mrk 3 are determined by the effects of the interaction between the radio-outflow and the ambient gas. In particular, along the radio-jet the line emitting gas shows two velocity systems separated by as much as 1700 km s $^{-1}$ which form broken velocity ellipsoids. This is a

clear indication that the gas is expanding away from the radio-jet axis and that the NLR is essentially a cylindrical shell expanding supersonically. These results are in close agreement with what we found in the NLR of other Seyfert galaxies observed with HST.

The physical picture which emerges is that the high velocity shocks induced by the outflowing plasma are heating and compressing the external gas. Close to the radio-jets, the gas is heated to a high temperature, 10^7 K, and thus forms a hot cocoon surrounding the jets. While its emission (mostly in the X-ray) can be relevant for the ionization properties of the NLR, it is negligible for the overall energy budget of the radio-source and thus the cocoon will undergo an essentially adiabatic expansion. During this expansion, it acts as a piston, accelerating and compressing the surrounding gas which is responsible for the narrow line emission. The jet kinetic energy is therefore transferred to the line emitting gas after it is dissipated in thermal energy associated with the cocoon.

With the current size of 200 pc the cocoon has expanded to several disk scale heights. The hot gas located above the plane of the disk is probably escaping into the halo, puncturing the bubble as indicated by the fractures in the velocity field. We believe that the NLR is currently in a momentum driven phase.

Aside from the highly perturbed gas associated with the radio-jet, a relatively quiescent component is also present, probably associated with the galaxy disk. The radio-outflow disrupts only locally its ordered rotation pattern.

In the framework in which the gas motions are driven by the radio-jets, it is possible to derive several key physical parameters describing the properties of the radio-source associated to Mrk 3. In particular, from the size of the cocoon and its lateral expansion speed we estimated an upper limit to its age ($\lesssim 1.5 \cdot 10^5$ years) and a lower limit to the jet kinetic power ($\gtrsim 2 \cdot 10^{42}$ erg s $^{-1}$). This provides quantitative support for

the proposed NLR model, since the total energy carried by the jet in its lifetime approximately equals the kinetic energy associated with the perturbed high velocity NLR gas, $\sim 6 \cdot 10^{54}$ erg.

Furthermore, if the advance speed of the Mrk 3 radio-source is taken to be representative, it implies that radio-outflows associated with Seyferts galaxies are short lived $\lesssim 10^5$ years, since their typical sizes are smaller than a few kpc.

Finally, while the jet kinetic luminosity of Mrk 3 is between 2 and 3 orders of magnitude smaller than that derived for radio-loud AGNs with similar emission line luminosity, the fraction of the jet power dissipated in radio-emission is similar to that of RL-AGN. We thus speculate that the main distinction between radio-quiet and radio-loud AGN is to be ascribed to a different jet power rather than to a different efficiency in producing synchrotron emission.

Exploring the effects of the jet propagation within the NLR of active nuclei is clearly a very promising tool to study the jet physics and to relate the properties of different classes of AGN. In particular it will be important to study the dynamical timescales for a statistically significant number of Seyfert and radio-galaxies to further test the proposed model.

REFERENCES

- Alexander, P., Leahy, J.P., 1987, MNRAS, 225, 1
- Axon, D.J., Capetti, A., Macchetto, F.D., 1998, ApJ submitted
- Axon, D.J., Marconi, A., Capetti, A., Macchetto, F.D., Schreier, E., A. Robinson, A., 1998, ApJL 496, 75
- Baldwin, J. A., Wilson, A. S. & Whittle, M., 1987, ApJ 319 84
- Becker, R.H., White, R.L., & Edwards, A.L., 1991 ApJS 75, 1
- Begelman, M., Cioffi, D.F., 1989, ApJL 345, 21
- Booler, R.V., Pedlar, A., & Davies, R.D., 1982, MNRAS 199, 229
- Bower, G., Wilson, A.S., Mulchaey, J., Miley, G.K., Heckman, T.M., and Krolik, J.H., 1994, AJ 107, 1686.
- Bower, G., Wilson, A.S., Morse, J.A., Gelderman, R., Whittle, M., and Mulchaey, J., 1995, ApJ 454, 106.
- Capetti, A., Macchetto, F.D., Sparks, W.B., Boksenberg, A., 1995a, ApJ 448, 600
- Capetti, A., Axon, D.J., Kukula, M., Macchetto, F., Pedlar, A., Sparks, W.B., & Boksenberg, A. 1995b, ApJL 454, L85
- Capetti, A., Axon, D.J., Macchetto F.D., Sparks, W.B., Boksenberg, A., 1996 ApJ, 469, 554.
- Capetti, A., Axon, D.J., & Macchetto, F.D., 1997a, ApJ 487, 560
- Capetti, A., Macchetto, F.D., & Lattanzi, M.G., 1997b, ApJL 476, L67
- Cox, D.P., Reynolds, R.J., 1987, ARA&A 25, 303
- De Young, D.S., 1993, ApJ 402, 95
- Dopita, M.A., Sutherland, R.S., 1995 ApJ 455, 468
- Dopita, M.A., Sutherland, R.S., 1996 ApJS 102, 161
- Falcke, H., Wilson, A.S., & Simpson, C., 1996, ApJL 470, L31
- Falcke, H., Wilson, A.S., & Simpson, C., 1998, ApJ 502, 199
- Gower, J.F.R., Scott, P.L. & Wills, D., 1967, MmRAS 71, 49
- Haniff, C. A., Wilson, A. S., & Ward, M. J., 1988, ApJ 334, 104

- Hartquist, T.W., Dyson, J.E., Pettini, M., Smith, L.J., 1986, MNRAS 221, 715
- Holloway, A.J., Steffen, W., Pedlar, A., Axon, D.J., Dyson, J.E., Meaburn, J., Tadhunter, C.N., 1996 MNRAS 279, 171
- Koski, A.T., 1978, ApJ 223, 56
- Kukula, M.J., Ghosh, T., Pedlar, A., Schilizzi, R.T., Miley, G.K., de Bruyn, A.G., Saikia, D.J., 1993, MNRAS 264, 893
- Kukula, M.J., Pedlar, A., Baum, S.A., O’Dea C.P., 1995, MNRAS 276, 1262 Liu, R., Pooley, G.G., Riley, J.M., 1992, MNRAS, 257, 545
- Macchetto, F. D., Marconi, A., Axon, D. J., Capetti, A., Sparks, W. B., Crane, P., 1997, ApJ 489, 579
- Mac Low, M.-M. & McCray, R., 1988, ApJ 324, 776
- Miller, P., Rawlings, P., & Saunders, R., 1993, MNRAS 263, 425
- Osterbrock, D.E., 1990, *Astrophysics of Gaseous Nebulae & Active Galactic Nuclei* (Mill Valley, CA: University Science Books)
- Parma, P., Murgia, M., Morganti R., Capetti, A., de Ruiter, H.R., Fanti, R. 1998, A&A submitted
- Pedlar, A., Unger, S.W., & Dyson, J.E., 1985, MNRAS 214 463
- Pedlar, A., Meaburn, J., Axon, D. J., Unger, S. W., Whittle, D. M., Meurs, E. J. A., Guerrine, N., & Ward, M. J., 1989, MNRAS 238, 863
- Pedlar, A., et al. 1993 MNRAS 263, 471
- Pogge, R.W., De Robertis, M.M., 1993, ApJ 404, 563
- Rawlings, P., Saunders, R., Eales, S.A., & MacKay C.D., 1989, MNRAS 240, 701
- Rawling, S., Sanders, R., 1991, Nature 349, 138
- Steffen, W., Holloway, A.J., Pedlar, A., 1996, MNRAS 282, 130
- Taylor, D., Dyson, J.E, Axon, D.J., & Pedlar, A., 1989, MNRAS 240, 487
- Taylor, D., Dyson, J.E, Axon, D.J., 1992, MNRAS 255, 351
- Tomisaka, K., Ikeuchi, S., 1986, PASJ 38, 697
- Ulvestad, J.S. & Wilson, A.S., 1984 ApJ 278 544
- Ulvestad, J.S. & Wilson, A.S., 1989 ApJ 343 659
- Wagner, S. J., 1987, A&A 185, 77
- Whittle, M., 1985, MNRAS 216, 817
- Whittle, M., Pedlar, A., Meurs, E.J.A., Unger, S.W., Axon, D.J., & Ward, M.J. 1988, ApJ, 326, 125
- Wilkins, T. W., Axon, D. J. 1992, in ASP Conf. 25, *Astronomical Data Analysis Software and Systems I*, ed. D. M. Worrall, C. Biemesderfer, & J. Barnes (San Francisco: ASP), 427
- Wilson, A.S. & Willis, A.G., 1980, ApJ 240, 429
- Wilson, A.S., & Ulvestad, J.S., 1983, ApJ 275, 8
- Wilson, A.S., Ulvestad, J.S., 1987 ApJ 319, 105
- Winge, C., Axon, D.J., Macchetto, F.D., Capetti, A., 1997, ApJL 487, 121
- Winge, C., Axon, D.J., Macchetto, F.D., Capetti, A., Marconi, A., 1998, ApJ submitted